

The Modern Universe As an Emergent State

Adam Weis

Abstract

The early universe was a hot, opaque soup of unbound fundamental particles. Our current universe is a cool transparent gas of bound atoms. What happened? In this paper, I will discuss our universe's cosmological history as a series of spontaneously-broken symmetries, and the resultant universe as an emergent state. The quark-hadron transition, nucleosynthesis, and recombination are discussed in terms of their thermodynamics and relevant order parameters. Concepts are compared with observations and experiments where relevant. I conclude with some (very) brief comments about structure formation.

Introduction

For a significant part of the cosmological history, the constituents of the universe were in close thermal contact, described more or less by a unique time-dependent temperature. After the Big Bang, our universe has continually expanded and its temperature has cooled. Along the way, the state of cosmological matter has changed radically from a quark-gluon plasma to bound atoms clustered via gravity. It seems reasonable that we might describe this current universe as an emergent phenomenon, characterized by several key phase transitions in its past. In this paper, I will describe these transitions primarily through equilibrium statistical physics, with two caveats:

- (1) The universe isn't really at equilibrium, it's expanding. This means that, as a correction to equilibrium methods, we must sometimes compare particle interaction rates to expansion rates in order to determine when equilibrium applies, and when certain phenomena are "frozen out" because the universe expands too rapidly for the relevant interactions to occur.
- (2) Our universe is hot. For much of its history it has had a relatively constant, high entropy, and many degrees of freedom per massive particle – 10^9 typically. This means that the long tails of Boltzmann distributions will be significant even when required interaction energies are significantly higher than thermal energies.

I will adopt the common convention of cosmology that $\hbar = k_B = c = 1$, giving mass, temperature, and energy equal units (I'll use eV). Note that the many critical phenomena are relevant to cosmology, and I do not intend my discussion to exhaust them. I will focus on three that I find interesting and relevant: the quark-hadron transition, nucleosynthesis, and recombination.

The Quark-Hadron Transition

At very early times when the universe is very dense and hot ($T > 1$ GeV), thermal energies are high enough that all matter is dissociated into quarks, leptons, and gauge bosons, the most fundamental particles in the Standard Model. Hadrons, matter composed of quarks bound by gluons, are not stable at these temperatures, and quarks roam free in an unbound state of matter called the quark-gluon plasma. As the universe expands and cools, thermal energies drop below the level necessary to sustain distantly separated quarks, and they bind into hadrons via the first-order quark-hadron transition [1].

One model [2] of this transition proposes the following Lagrangian density:

$$L = i\bar{\psi}\gamma^\mu\partial_\mu\psi + \frac{1}{2}\partial_\mu\xi\partial^\mu\xi + \frac{1}{4}\xi^2\text{Tr}(\partial_\mu U\partial^\mu U^\dagger) - g\xi(\bar{\psi}_L U\psi_R + \bar{\psi}_R U^\dagger\psi_L) - V_T(\xi)$$

where U is an element of the group $SU(2)$ and γ is a Dirac matrix. I will not attempt to explain this Lagrangian in full. It is based on the so-called Lee-Wick model [3] in which particles are confined by a scalar field σ , but includes an additional isovector field π and a term with coupling constant g that introduces chirality. The parameter ξ is related to these fields by:

$$\xi U = \sigma + i\tau \cdot \pi \quad \text{and} \quad \xi = (\sigma^2 + \pi^2)^{1/2}$$

Notice then, that ξ is effectively a measure of the strength of the quark-confining fields. The quark field $\psi = (\psi_L, \psi_R)$ is expressed in terms of "left-handed" and "right-handed"

components. Finally, the potential $V_T(\xi)$ at finite temperature looks like:

$$V_T(\xi) = \frac{1}{2}f_\pi^2 \left(\lambda^2 - \frac{12B}{f_\pi^4} \right) \xi^2 \left(1 - \frac{\xi}{f_\pi} \right)^2 + B \left(1 + 3 \left(\frac{\xi}{f_\pi} \right)^4 - 4 \left(\frac{\xi}{f_\pi} \right)^3 \right) - \frac{24}{2\pi^2} T^4 \int_0^\infty x^2 dx \ln \left(1 + e^{-\sqrt{x^2 + (g\xi/T)^2}} \right)$$

This potential is based on various "bag models" [4] which effectively consider hadrons as quarks confined by a volumetric pressure (second term) and surface tension (first term), as if bound by a plastic bag; the third term determines temperature dependence. These large equations tend to obscure the physics, but we observe that plotting the potential V_T as in Figure 1 reproduces the behavior expected for a first-order phase transition. The two dashed curves represent potentials for temperatures just above, and just below a critical temperature T_c as a function of the order parameter ξ/f_π . As T goes below T_c , the global potential minimum suddenly jumps from $\xi/f_\pi = 0$ to $\xi/f_\pi = 1$, indicating a phase transition. The $\xi/f_\pi = 0$ point remains stable, and is separated from the $\xi/f_\pi = 1$ point by a potential barrier, indicating that this transition is first-order and has non-vanishing latent heat. Because this transition is first-order, it is prone to the formation of domain walls, which are topologically metastable. The quark-hadron transition proceeds slowly via nucleating hadronic bubbles after some amount of supercooling, so estimates of the critical temperature vary, but are typically quoted to be on the order of 100 MeV [1].

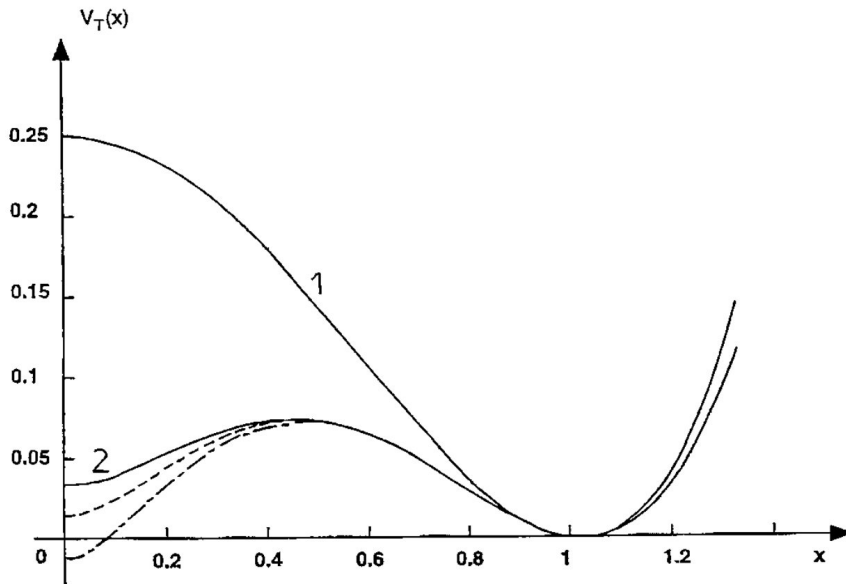


FIGURE 1. Potential $V_T(x) = V_T(\xi)/(\frac{1}{2}f_\pi^4\lambda^2)$ for quark-hadron transition as a function of the order parameter $x = \xi/f_\pi$. Curves 1 and 2 are for different parameters $\{f_\pi, B, \lambda\}$. The dotted line is for $T = 0.9T_c$ and the dash-dot line is for $T = 1.1T_c$. Cooling to the critical temperature, the potential minimum shifts from 0 to 1, but the $x = 0$ point remains stable, suggesting a first order transition.

Phase transitions such as the one depicted in Figure 1 usually suggest a spontaneously-broken symmetry. From the Lagrangian L discussed above, we can be explicit about what symmetry, exactly, is broken in this case. The two terms of interest are the first term, $i\bar{\psi}\gamma^\mu\partial_\mu\psi$ and the cross term, $g\xi(\bar{\psi}_L U\psi_R + \bar{\psi}_R U^+\psi_L)$. First, notice that regardless of the value of ξ , L is symmetric under transformations of the type:

$$\begin{pmatrix} \psi_R \\ \psi_L \end{pmatrix} \rightarrow \begin{pmatrix} e^{i\theta}\psi_R \\ e^{i\theta}\psi_L \end{pmatrix} \quad \text{or} \quad \begin{pmatrix} \psi_R \\ \psi_L \end{pmatrix} \rightarrow \begin{pmatrix} e^{i\theta}\psi_R \\ e^{-i\theta}\psi_L \end{pmatrix}$$

for arbitrary θ . Hence the quark-hadron transition preserves two distinct $U(1)$ symmetries. Now consider a chiral transformation that rotates between left- and right-handed quarks:

$$\psi = \begin{pmatrix} \psi_L \\ \psi_R \end{pmatrix} \rightarrow \begin{pmatrix} \cos\theta & -\sin\theta \\ \sin\theta & \cos\theta \end{pmatrix} \begin{pmatrix} \psi_L \\ \psi_R \end{pmatrix} = \begin{pmatrix} \psi_L \cos\theta - \psi_R \sin\theta \\ \psi_L \sin\theta + \psi_R \cos\theta \end{pmatrix}$$

In the high-T deconfined phase, $\xi = 0$ and only the first term appears in the Lagrangian. This term is unaffected by the chiral transformation, since:

$$\psi\bar{\psi} \rightarrow \left| \begin{pmatrix} \psi_L \cos\theta - \psi_R \sin\theta \\ \psi_L \sin\theta + \psi_R \cos\theta \end{pmatrix} \right|^2 = |\psi_L|^2 + |\psi_R|^2 = \psi\bar{\psi}$$

However, in the low-temperature confined phase, $\xi/f_\pi = 1$, and we must also consider the cross term. This term is not preserved under the transformation:

$$\begin{aligned} \bar{\psi}_L U\psi_R + \bar{\psi}_R U^+\psi_L &\rightarrow (\bar{\psi}_L \cos\theta - \bar{\psi}_R \sin\theta)U(\psi_L \sin\theta + \psi_R \cos\theta) + \dots \\ &\neq \bar{\psi}_L U\psi_R + \bar{\psi}_R U^+\psi_L \end{aligned}$$

Hence, the high-temperature phase has two $SU(2)$ symmetries (I've only shown one here, but the other is similar), while the low-temperature phase has neither. In summary, the transition from the deconfined high-temperature phase to the confined hadronic low-temperature phase corresponds to a reduction of the lagrangian's symmetry group with respect to ψ :

$$U(1) \otimes U(1) \otimes SU(2) \otimes SU(2) \rightarrow U(1) \otimes U(1)$$

This is known as chiral symmetry breaking, because the low-T confined phase distinguishes between left-handed quarks ψ_L and right-handed quarks ψ_R , while the high-T quark-gluon plasma phase does not.

We can see that the breaking of chiral symmetry is exactly what *should* happen when once-free quarks are confined. First, recall that chirality has the same intuitive meaning for quarks as it does for the more familiar photons – if a quark has angular momentum or magnetic moment parallel to its momentum it is said to be left-handed and if antiparallel, it is right-handed. Now consider the intuitive picture suggested by the bag model [4] of a hadron. If a quark bounces off of the sharp potential boundary (the "bag") at the edge of the hadron, its momentum will flip signs but its magnetic moment will stay the same and its chirality will change. Unconfined quarks in a quark-gluon plasma do not reflect in this matter and their chirality is a conserved quantity.

It is of interest that the high-temperature quark-gluon plasma phase has supposedly been created in accelerator experiments that collide heavy ions, such as SPS-CERN, RHIC, and the soon-to-be-running ALICE at the LHC [5]. These experiments collide ions at high enough energies that most incident nucleons are carried away, but deposit an enormous energy density in the region of collision in the form of quark and gluons. Several particle

signatures are cited as evidence of a quark-gluon plasma, one of which is the suppression of the charmonium or " J/ψ " state, a bound state of a charm and an anti-charm quark. These particles are produced in the early stages of Pb-Pb collisions at SPS. Charmonium has a lifetime greater than the quark-gluon plasma state itself, and decays into leptons that don't interact with the plasma, so it is capable of probing the quark-gluon state. At low energy densities, the J/ψ state is normally suppressed by interactions with nucleons. Roughly speaking, at higher energy densities the suppressing nucleons are instead transformed into deconfined quarks and gluons, and lesser J/ψ is observed. This data is shown in Figure 2. More recent data from RHIC has also suggested the presence of a strongly-coupled quark-gluon phase [6]. Furthermore, from elliptic flow experiments using collisions with non-zero impact parameter, studies at RHIC suggest that the quark-gluon plasma behaves as an extremely low-viscosity fluid. This notion is consistent with the idea of the early phase of the universe as a rapidly thermalizing state of matter.

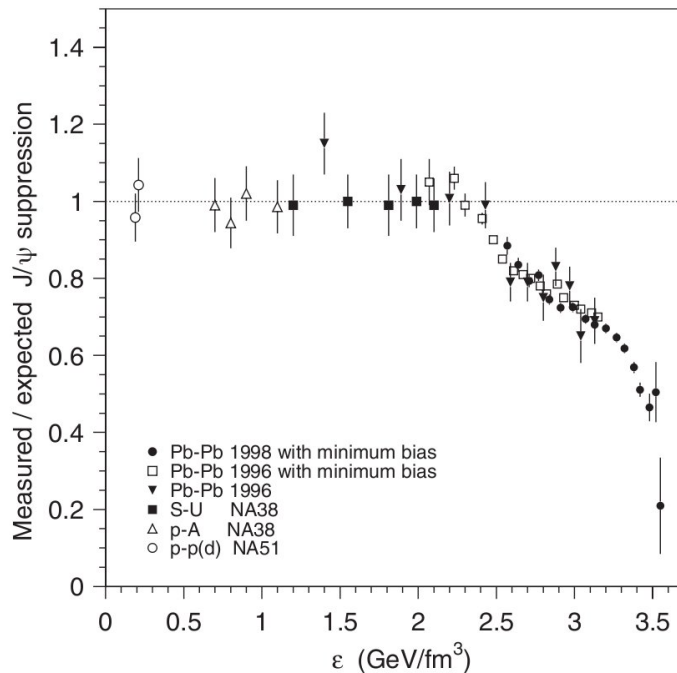
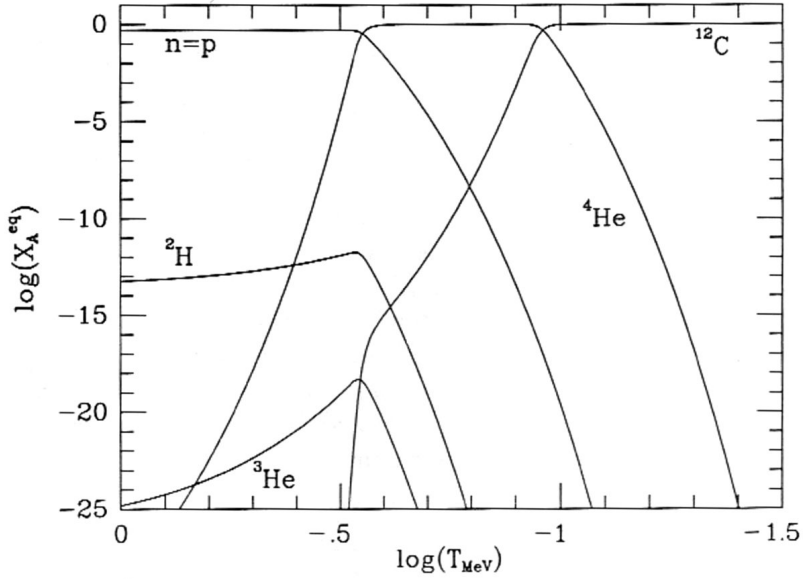


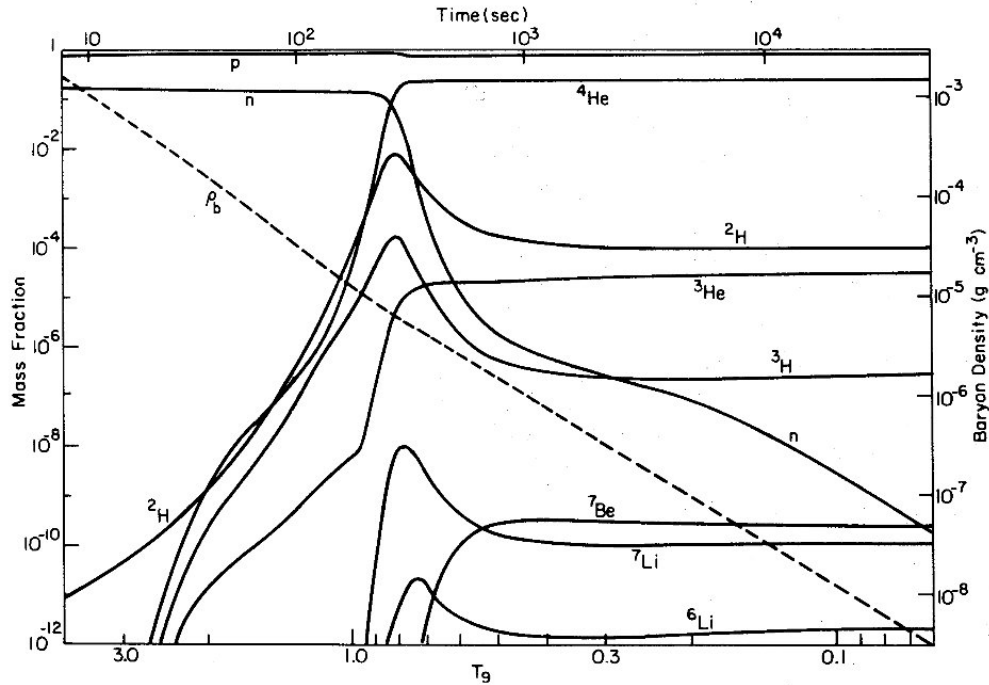
FIGURE 2. Charmonium suppression as a function of energy density ϵ , from SPS-CERN experiment. As predicted, charmonium is suppressed less at high energy densities where the quark-gluon plasma is produced.

Nucleosynthesis

At temperatures less than 1 MeV, the universe is cool enough that protons and neutrons will begin binding into light nuclei, a process known as Big-Bang Nucleosynthesis (BBN). At $T \lesssim 1$ eV, the rate of weak interactions falls below the universe's expansion rate, "freezing in" the ratio of neutrons to protons, and shortly afterwards nucleons begin binding into D (^2H), ^3H , ^3He , and ^4He , in order of increasing mass number and binding energy [7].



(a) Mass fractions X_A^{eq} of nuclei species from statistical equilibrium model. Suggests interpreting X_A^{eq} as order parameters. The dominant phases with decreasing temperature would be free nucleons, helium, and then heavier elements. The dominance of ^{12}C over H and ^4He is not observed in our universe, suggesting that non-equilibrium effects became important before a low-temperature equilibrium was obtained.



(b) Numerical non-equilibrium calculation of mass fractions, as functions of temperature T in MeV. Mass fractions "freeze in" with H and ^4He dominant

FIGURE 3

Clearly, one of the most important initial conditions of the nucleosynthesis epoch will be the ratio of the neutrons to protons n/p , a parameter moderated by weak interactions such as beta decay. If these interactions occur at a rate Γ_{np} higher than the rate of expansion H , neutrons and protons attain chemical equilibrium, and their ratio is given by the Boltzmann distribution:

$$\left(\frac{n}{p}\right)_{\text{EQ}} = \exp\left(-\frac{m_n - m_p}{T}\right)$$

where $m_n - m_p = 1.293$ MeV is the neutron-proton mass difference. At the beginning of nucleosynthesis, this equilibrium no longer holds because $\Gamma_{np} < H$, and n/p is "frozen" into its value at the temperature where the equilibrium condition $\Gamma_{np} \gtrsim H$ last held. Computing Γ_{np} by integrating the beta-decay matrix element over phase space, and H by Hubble's Law it can be shown [8] that:

$$\frac{\Gamma_{np}}{H} \sim \left(\frac{T}{0.8 \text{ MeV}}\right)^3$$

Hence, $T \sim 0.8$ MeV is the temperature where n/p stabilizes. By our equilibrium equation, $(n/p) \sim \exp(-1.293/0.8) = 1/6$ when neutrons and protons are mostly decoupled. Neutrons will continue slowly beta-decaying into protons for a while, so $n/p = 1/7$ is the appropriate initial condition for nucleosynthesis.

Armed with this initial condition, it is possible to calculate the mass fractions X_A of various light nuclei, denoted by mass number A and atomic number Z . Assuming nonrelativistic statistical equilibrium between nuclei species it follows that:

$$X_A = \frac{n_A A}{n_n + n_p + \sum_i (A n_A)_i} = \frac{g_A}{2} \left[\frac{\zeta(3)}{\sqrt{\pi}} \eta \left(\frac{2T}{m_N}\right)^{3/2} \right]^{A-1} A^{5/2} X_p^Z X_n^{A-Z} \exp\left(\frac{B_A}{T}\right)$$

where g_A counts internal degrees of freedom, η is the baryon-to-photon ratio, $m_N \equiv m_n \approx m_p$ is the nucleon mass, and $B_A = Zm_p + (A - Z)m_n - m_A$ is the binding energy. These equilibrium mass fractions, as functions of temperature are shown in Figure 3(a) [8]. The rapid variation of mass fractions shown by this model suggest considering bound nuclei as an emergent state, with X_A as order parameters for distinct phases that compete over the temperature range shown. However, the dominance of heavier isotopes, represented by ^{12}C in Figure 3(a), is very different from the universe we observe today, suggesting that non-equilibrium effects are extremely important in correctly predicting elemental abundances.

In general, accurate abundances for the non-equilibrium expanding universe are calculated known matrix elements and cross sections, with each interaction rate for a given species depending on the existing abundances of other species. Comparing these rates, with mind to temperature and expansion, gives a set of differential equations that can be solve numerically for abundances as a function of temperature, as shown in Figure 3(b) [9]. Although abundance computation is quite tricky, we can easily estimate the ^4He mass fraction by assuming all neutrons are in ^4He :

$$X_4 = \frac{4n_4}{n_N} = \frac{4\frac{n_n}{2}}{n_n + n_p} = \frac{2\frac{n}{p}}{1 + \frac{n}{p}} = 25\%$$

using the $n/p = 1/7$ result from above. This approximation is consistent with more refined models and observation. The assumption that all neutrons are in ^4He is reasonable because ^4He has the highest binding energy of all the light elements. Because no stable nuclei exist

with $A = 5$ or 8 – phenomena known as "mass gaps" – synthesis of heavier nuclei can't proceed by accumulation of free neutrons, but must involve interactions among existing D, ^3H , ^3He , and ^4He which are unlikely due to Coulomb repulsion. Heuristically then, we should expect the vast majority of the universe to be in the form of tightly bound ^4He and leftover H, with small amounts of D, ^3H , ^3He , trace amounts of ^6Li , ^7Li , and ^7Be and very little of any other extra-stellar nuclear species. This is consistent with the calculated results shown in Figure 3(b) and Figure 4.

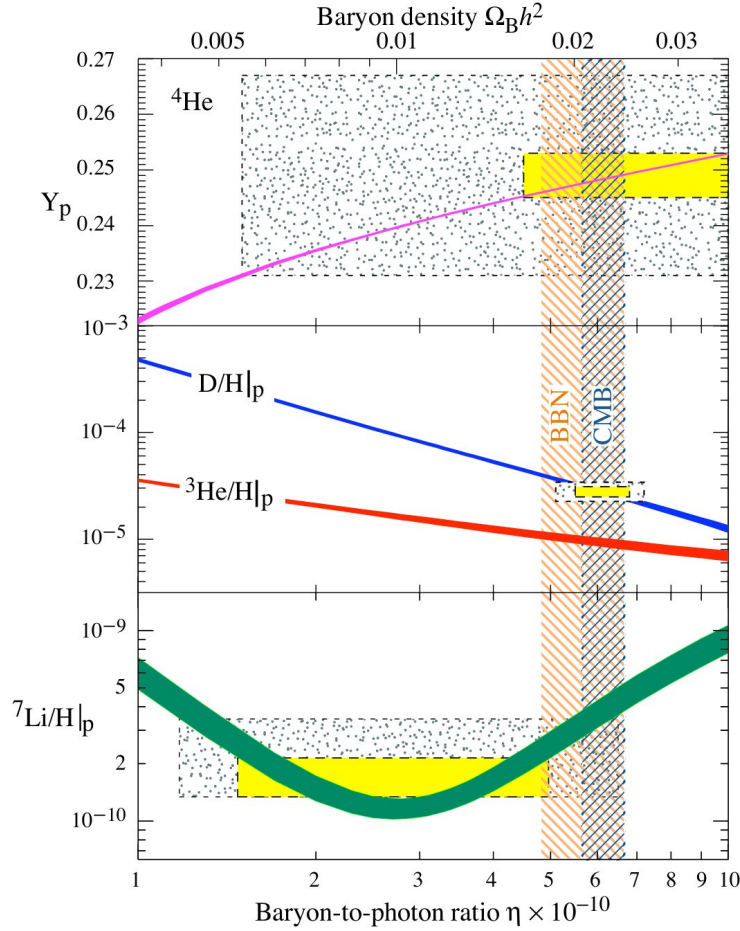


FIGURE 4. Mass fraction predictions with η dependence. Thickness of lines is from uncertainties in nuclear reaction parameters. Yellow boxes are estimates/constraints from observational astronomy (not necessarily the same observations discussed in text), green boxes are with more conservative errors. Orange bar shows overall estimate of η from comparison of BBN model to observed abundances. Blue bar is independent estimate from cosmic microwave background.

Figure 4 shows the dependence of abundance computations on the baryon-to-photon ratio η [10]. The thickness of the lines indicate uncertainties in cross sections for the relevant nuclear interactions. The dependence on η suggests that sensitively measuring primordial abundances of nuclei would effectively measure the baryon-to-photon ratio, which is difficult

to determine directly. These primordial elemental abundances have been partially obscured by more recent stellar processes that produce or destroy the nuclei in question. Hence, from the perspective of our current universe, measurement of primordial abundances requires careful selection of objects, usually old high-redshift entities, that should have preserved the element in question. Some of these results are summarized below:

- *Deuterium*: Deuterium is an ideal probe of the nucleosynthesis epoch because it is thought to be produced almost exclusively in the big bang, and only very rarely in stellar processes [11]. Hence it is only destroyed, and any observation, even local ones, set a lower bound on primordial deuterium levels. D/H ratios thought to be primordial have been measured by observing deuterium absorption spectra in quasars with redshifts $z \approx 2.52$ [12]. Notice that the deuterium and hydrogen have slightly different spectra because their quantum energy levels depend on their reduced electron-nucleus masses, which are slightly different. This data suggests $D/H = 2.78_{-0.38}^{+0.44} \times 10^{-5}$ and $\eta = 5.9 \pm 0.5 \times 10^{-10}$, as shown in Figure 4.
- *Helium 4*: ${}^4\text{He}$ abundance has been measured using spectroscopic observations of blue compact galaxies [13]. The stars in these galaxies emit mostly in the blue and UV range, and their metallicity – measured by oxygen absorption spectra – is low, suggesting that they are young, and stellar processes have begun only recently. Therefore, their abundances should be close to primordial. The mass fraction of ${}^4\text{He}$ from this data is $Y_p = 0.2421 \pm 0.0021$. Note that because ${}^4\text{He}$ is frequently produced and consumed by stellar fusion, and because its abundance has only weak η dependence, it is not the preferred method of probing BBN.
- *Lithium 7*: Lithium abundance has been measured by observing a hand-selected group of 23 low-metallicity objects [14]. The from the data presented, it can be estimated $Li/H \approx 1.12 \pm 0.12 \times 10^{-10}$, although the authors caution that their data still shows a correlation between Li/H and metallicity, suggesting that this value is non truly primordial.

In summary, deuterium observations constrain the value of η tightly, and ${}^4\text{He}$ and ${}^7\text{Li}$ observations are qualitatively consistent, but quantitatively problematic. Of all observations of primordial abundances, lithium is perhaps the most problematic because its η -dependence is non-monotonic, as shown in Figure 4 and it is known that certain stars produce non-trivial amounts of Li. The projections of η from these independent abundance measurements are not ideally consistent either with each other or other η projections from cosmic microwave background measurements. These observations are prone to systematic errors due to unaccounted for astrophysical processes, and these measurements suggest that a better understanding of stellar production rates etc. will be necessary to probe BBN in greater detail.

It should be noted however, that although abundance measurements determine η only poorly, their magnitudes agree very well with the range of values predicted by the model depicted in Figures 3(b) and 4. These predictions required an initial condition of thermal equilibrium among nuclear species, and also non-equilibrium effects due to expansion. For this reason the body of data on primordial nuclear abundances, is considered perhaps the strongest existing evidence of the big-bang model.

Recombination

When the hot plasma universe cools to thermal energies on the order of 1 eV, light atomic nuclei and electrons will begin binding into neutral atoms, a process known as "recombination." At $T \approx 1$ eV, mass energies of relevant particles greatly exceed thermal energy and we can use nonrelativistic limits of Bose-Einstein and Fermi-Dirac statistics. Assuming the electrons bind predominantly into the ground state of hydrogen, the equilibrium number density of atomic hydrogen will be[15]:

$$n_H = \frac{g_H}{g_p g_e} n_p n_e \left(\frac{m_e T}{2\pi} \right)^{3/2} \exp\left(\frac{B}{T}\right)$$

where $B = m_p + m_e - m_H$ is the binding energy of hydrogen. Defining the fractional ionization $X_e = n_p/n_B$, we can turn the above result into the Saha equation for the equilibrium ionization:

$$\frac{1 - X_e}{X_e^2} = \frac{4\sqrt{2}\zeta(3)}{\sqrt{\pi}} \eta \left(\frac{T}{m_e} \right)^{3/2} \exp\left(\frac{B}{T}\right)$$

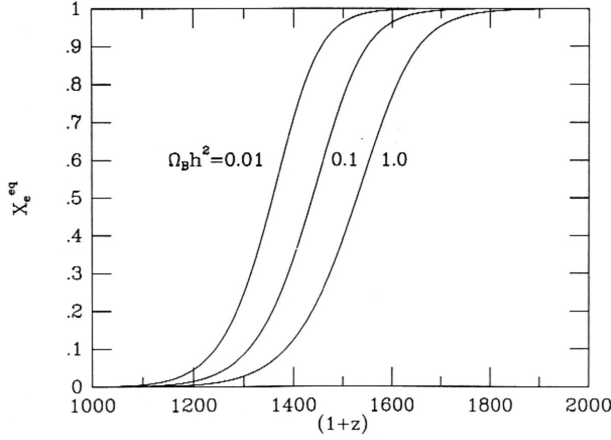
where $\eta = 2.68 \times 10^{-8} (\Omega_B h^2)$ is the baryon-to-photon ratio. Recall that h is the dimensionless Hubble's constant and $\Omega_B = 8\pi G \rho_B / 3H^2$ is the ratio of baryonic mass density to the critical density needed for flat spacetime. The fractional ionization as a function of redshift[15, 16] is shown in Figure 5(a) and 5(c). Recall that in an expanding universe, large redshifts are related to time by [17]:

$$t(z) = \frac{2}{3H_0 \Omega_0^{1/2} z^{-3/2}}$$

The sharp transition of X_e from 0 to 1 at a particular redshift indicates that we might think of the recombination transition of the universe as a phase transition, with X_e as an order parameter. It is likely that this transition is first order, considering similar transitions observed in plasma experiments [18], theoretical equations of state [19], and signature nucleation bubbles seen in simulations of ionization transitions [20]. If we take $X_e < 0.1$ as the threshold for a deionized universe, then we can use the above transcendental equation to find the critical temperature of recombination. This critical temperature is approximately $T_{\text{rec}} \approx 0.308$ eV or 3575 K, but is weakly dependent on $\Omega_B h^2$ as shown in Figure 5(b). Notice that the critical thermal energy for recombination is significantly lower than the binding energy of hydrogen, counterintuitively. This discrepancy occurs primarily because the number of photons greatly exceeds the number of baryons in the universe, as evidenced by $\eta \sim 3 \times 10^{-9}$. Hence, even when $T_{\text{rec}} \lesssim 13.6$ eV, the high-energy Boltzmann tail of the photon distribution still effectively ionizes any atoms and the temperature must drop further for large-scale recombination.

The equilibrium transition, shown as the dotted line in Figure 5(c), is extremely sharp, but including the non-equilibrium correction that the universe is expanding (dashed lines and solid line) slows the transition slightly. This, and other non-equilibrium corrections, also "freeze in" a residual ionization at late times, when the universe expansion rate exceeds the rate at which free charges collide and form atoms.

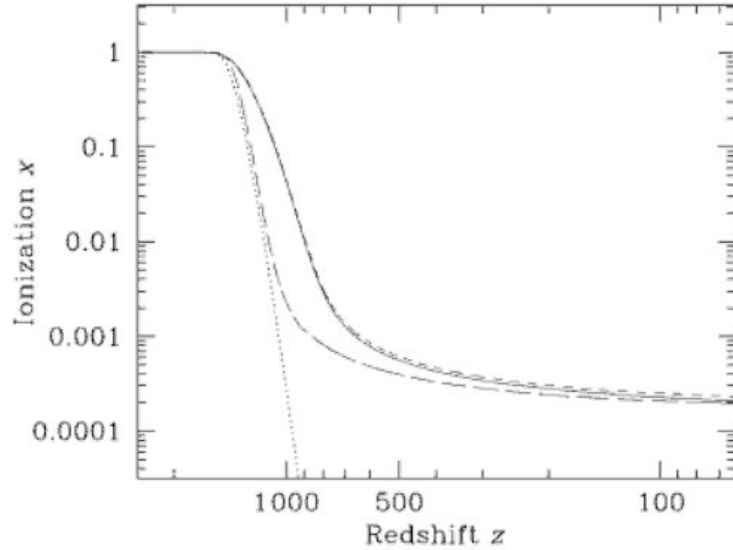
The recombination process leads to qualitative changes in the universe beyond the microscopic state of its matter, particularly the decoupling of matter and radiation. Near the recombination epoch, photons interact much more strongly with charged matter, such



(a) Ionization fraction X_e^{eq} as a function of redshift z from a statistical equilibrium model. Notice weak $\Omega_B h^2$ dependence

$\Omega_B h^2$	T (eV)
0.01	0.2908
0.10	0.3064
1.00	0.3239

(b) Critical temperatures for deionization, calculated with Saha equation in Mathematica.



(c) Residual ionization as function of redshift. In increasing order of model accuracy: *Dotted line* – Saha equilibrium model. *Long dashes* – non-equilibrium calculation with expansion. *Short dashes* – expansion and correction for reionization by Lyman α photons. *Solid line* – expansion, Lyman α , and correction for decoupling of ion and photon temperatures

FIGURE 5

as free electrons, than with neutral atoms. The interaction rate of photons is $\Gamma_\gamma = \sigma_T n_e$ where n_e is the density of free electrons and $\sigma_T = 6.65 \times 10^{-25}$ is the Thomson scattering cross section. As electrons bind into atoms, n_e and Γ_γ decrease significantly and the mean free path of photons increases enormously – the universe becomes transparent. One consequence of this emergent transparency is that, if we observe photons in our current universe, some portion of them will have last scattered immediately before recombination, when the

universe was a thermalized opaque plasma. This thermal radiation is the famous cosmic background radiation (CMB) first observed by Penzias and Wilson [21] and now being studied in the WMAP experiment [22]. The isotropy of this radiation, and its remarkably close agreement to a Planck spectrum confirm its thermal origin, and more generally confirm the Big-Bang model. WMAP and other projects measure the current temperature (via the peak wavelength) of this radiation as 2.725 K, which when combined with an estimate of the CMB redshift via Hubble’s constant, gives an estimate of the temperature at recombination, since $T_{\text{then}}/T_{\text{now}} = 1 + z$. This recombination temperature in turn depends on η or $\Omega_B h^2$ as discussed above. Hence, precise measurement of the CMB temperature determines a curve in the space $\{H_0, \eta\}$, that along with much other data is used in WMAP’s computations of cosmological parameters and their constraints. This is the source of the CMB determination of η shown in Figure 4.

Conclusions and Comments about Structure Formation

Up to this point, I have discussed the cosmological phase transitions of hadronization, nucleosynthesis, and recombination from the perspective of order parameters and emergent states. Calculations included the broken symmetry of the quark-hadron transition, estimation ^4He abundance, and computation of critical temperatures for recombination. This narrative traces the history of the early universe from a hot, opaque quark-gluon plasma to a cooler, transparent gas of bound atoms. Clearly the characterization of our current universe as emergent is accurate, however it would be incomplete to neglect our universe’s most recent emergent phenomenon – galaxies and large scale structure. A detailed discussion of this is beyond this paper’s scope, but I will make comment briefly.

Perhaps the most interesting thing about the formation of galaxies, galactic clusters, and other large scale structures is that these phenomena were in large part seeded by the transitions already discussed. When the universe was opaque, photon scattering was frequent and radiation pressure competed with gravitational forces, but as recombination began, photons interacted less strongly with matter, radiation pressure decreased, and gravitational forces began clustering atoms into the structures we observe today [23]. The dominance of gravitational pressure over radiation enabled the amplification of existing inhomogeneities, some of which may have been consequences of inhomogeneous nucleation during the first-order quark-hadron and recombination transitions.

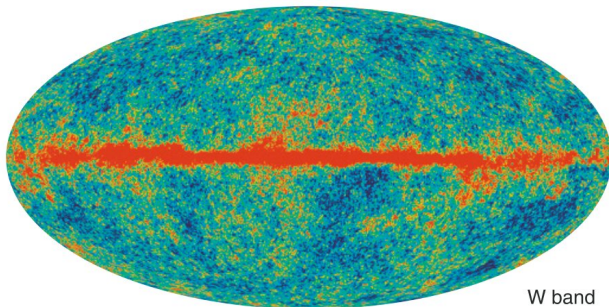


FIGURE 6. Sky map of fluctuations (one part in a thousand) from isotropic CMB temperature at 94 GHz

Notice that the initial growth of inhomogeneity requires only that gravitational forces exceed radiation pressure, not that radiation pressure vanish. Hence, structure formation requires only partial recombination, and begins shortly *before* the emergent transparency that causes the cosmic microwave background. The CMB, therefore, is a snapshot of a universe in which structure formation has already begun. CMB anisotropies, as measured precisely by WMAP [24] and shown in Figure 6 offer a map of the inhomogeneities that would become the structure we observe today. The modern universe, from galactic clusters to atoms, nuclei, and hadrons, is a consequence of emergent phenomena.

REFERENCES

- [1] B. W. Mintz et al. On the nucleation of hadronic domains in the quark-hadron transition. *Nuc. Phys. A*, 820:291c–294c, 2009.
- [2] W. N. Cottingham and R. V. Mau. Quark hadron phase transition in models with chiral symmetry. *J. Phys. G: Nucl. Part. Phys.*, 24:1227–1233, 1998.
- [3] T. D. Lee and G. C. Wick. Vacuum stability and vacuum excitation in a spin-0 field theory. *Phys. Rev. D*, 9:2291, 1974.
- [4] E. J. Squires. The bag model of hadrons. *Rep. Prog. Phys.*, 42:071187, 1979.
- [5] D. Boyanovsky et al. Phase transitions in the early universe. *Annu. Rev. Nucl. Par. Sci.*, 56:441–500, 2006. see section: Studying Phase Transitions with Accelerators.
- [6] U. W. Heinz. The quark-gluon plasma at rhic. *Nuc. Phys. A*, 721:30–39, 2003.
- [7] G. Steigman. Primordial nucleosynthesis: Successes and challenges. *Int. J. Mod. Phys.*, E15:1–36, 2006.
- [8] E.W. Kolb and M.S. Turner. *The Early Universe*, chapter Big-Bang Nucleosynthesis. Addison-Wesley Publishing Co, 1990.
- [9] R.V. Wagoner. Big-bang nucleosynthesis revisited. *Astrophys. J.*, 179:343–360, 1973.
- [10] W.-M. Yao et al. Big-bang nucleosynthesis. *Journal of Physics G*, 33:1, 2006.
- [11] G. Steigman. Bbn and the primordial abundances. In *Proceedings of the ESO/Arceti Workshop on Chemical Abundances and Mixing in Stars in the Milky Way and its Satellites*, ESO Astrophysics Symposia. Springer-Verlag, 2005.
- [12] D. Kirkman et al. The cosmological baryon density from the deuterium to hydrogen ratio towards qso absorption systems: D/h towards q1243+3047. *Astrophys. J. Sup.*, 149:1, 2003.
- [13] Y.I Izotov and T.X. Thuan. Systematic effects and a new determination of the primordial abundance of ^4he and dy/dz from observations of blue compact galaxies. *Astrophys. J.*, 602:200–230, 2004.
- [14] S. G. Ryan J. E. Norris and T. C. Beers. The spite lithium plateau: Ultrathin but postprimordial. *Astrophys. J.*, 523:654–677, 1999.
- [15] E.W. Kolb and M.S. Turner. *The Early Universe*, pages 78–79. Addison-Wesley Publishing Co, 1990.
- [16] M. Stiavelli. *From First Light to Reionization: The End of the Dark Ages*, page 12. Wiley-VCH, 2009.
- [17] M.S. Longair. *Galaxy Formation*, page 161. Springer, 1998.
- [18] V.F. Kozhvnikov et al. A first-order transition in mercury vapor. *J. Phys.: Condens. Matter*, 6:A249–A254, 1994.
- [19] D. Beule et al. Hydrogen equation of state and plasma phase transition. *Contrib. Plasma Phys.*, 39:1–2, 21–24, 1999.
- [20] V. S. Filinov et al. Phase transition in strongly degenerate hydrogen plasma. *JETP Letters*, 7:384–387, 2001.
- [21] A. A. Penzias and R. W. Wilson. A measurement of excess antenna temperature at 4080 mc/s. *Astrophys. J.*, 142:419–421, 1965.
- [22] E. Komatsu et al. Five-year wilkinson microwave anisotropy probe observations: Cosmological interpretation. *Astrophys. J. Sup.*, 180:330–376, 2009.
- [23] M. J. Rees. The emergence of structure in the universe. *Il Nuo. Cim.*, 107 A:1045–1061, 1994.
- [24] G. Hinshaw et al. Five year wilkinson microwave anisotropy probe observations: Data processing, sky maps, and basic results. *Astrophys. J. Sup.*, 180:225–245, 2009.